Study on fabrication and Characterization of NANO iron and Nano Iron on Carrier

Nguyen Hong Anh[1], Uong Van Vy[2], Nguyen Thi Lan Anh[3], Tran Van Chung[4*], Le Xuan Que[5]

[1,3,5]Institute of Energy Science, VAST
[2,5]Institute for Tropical Technology, VAST
[*4]Institute of Chemistry and Material, 17 Hoang Sam Hanoi
*Corresponding author: tranchunghhvl@gmail.com

Abstract— *Gasification of biomass fabricating syngas fuels has contributed to expand the applicability of solid biomass fuel. But the by-product tar of the gasification has largely limited the effectiveness. However, gasification Fe- catalyst has been recognized as a good factor reducing the tar and increasing the gas quality. The paper studies the fabrication of separated nano iron and carrier attached nano iron regarding to a catalytic application during the biomass gasification. The applied technique of the fabrication includes pyrolysis and mechanical milling. Character of the products, as structures and particle dimension, has been examined. The suitable fabrication condition has been considered.*

Keywords— Nano Iron, Pyrolysis, Milling, Fabrication technique, Gasification of Biomass Fabrication.

I. INTRODUCTION

Biomass energy is renewable, estimated to provide 10% to 14% of energy needs. Gasification, pyrolysis of biomass is an emerging technology research in the world to bring about the development of sustainable clean energy systems, reduce dependence on fossil fuels [1-6]. However, the biomass gasification is not only useful, but also has some unwanted byproducts. Among them, the tar is considered to be one of the most pressing issues in any gasification system. High concentrations of tar may cause damage or lead to destruction of turbine and engines.

Tars may be removed by using catalysts [1-5]. Catalytic methods can be classified as restructuring, cracking, hydrogenation and oxidation selectivity. To increase energy efficiency, tar removal process should perform in the temperature range from 350 ° C to 700 ° C. Mechanism of reaction decomposing tar was studied, for example, by Simell et al. [1], using toluene as an ingredient of tar in hot air. A series of decomposition reactions of tar have been proposed, generally similar to the process of cracking. Recently iron catalyst to attract the attention of many researchers [7]. The most attractive iron catalytic material has been fabricated using nano technology, including thermal reduction in H_2 atmosphere and mechanical milling. In addition, iron powder studied in this paper in general is strong reducer applicable for many fields, especially for remediation of contaminated water and soil with persistent organic pollutants [8 – 10], and also for fabrication of oxygen scavenger [11].

II. EXPERIMENT

2.1 Methods

2.1.1 Fabrication of nano iron powder

The powder was reduced from solgel oxide using pyrolysis in hydrogen atmosphere. Hydrogen generator is electrochemical in a tank 70 liters with alkaline electrolyt at current 20A. H_2 gas product vas dried then conduit into 1kW electric furnace with controllable temperature up to 900^{o}C. The reactor is quartz tube diameter 25 mmx100 mmx120 mm. The gas conductors in the system were controlled by suitable valves to ensure the fire safety.

Diagram block of nano iron fabrication process by hydrogen reducing method at high temperatures is shown in Figure 1.

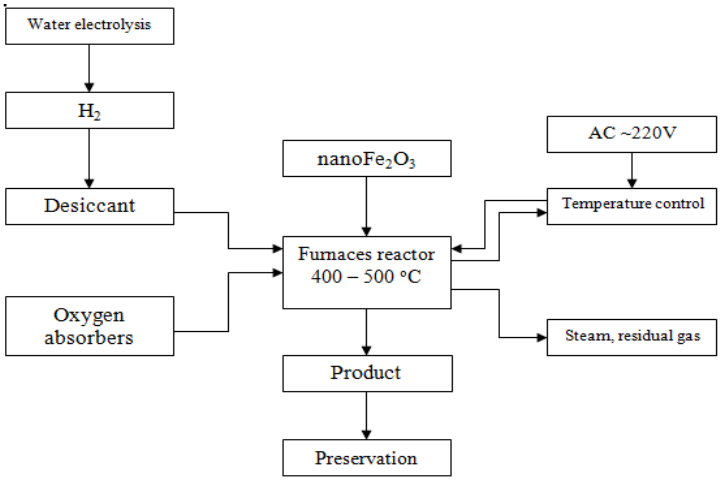

FIGURE 1. DIAGRAM OF PROCESS EQUIPMENTS FOR NANOMETER IRON FABRICATION

2.1.2 Mechanic Milling

The Fritsch P-6 planetary ball mill has four milling stations in which a few hundred grams of the powder can be milled at a time. The planetary ball mill owes its name to the planet-like movement of its vials. These vials are arranged on a rotating support disk and a special drive mechanism causes them to rotate around their own axes. The centrifugal force produced by the vials rotating around their own axes and that produced by the rotating support disk both act on the vial contents, consisting of material to be ground and the grinding balls. Since the vials and the supporting disk rotate in opposite directions, the centrifugal forces alternately act in forward and opposite directions. This causes the grinding balls to run down inside the wall of the vial - the friction effect, followed by the material being ground and grinding balls lifting off and traveling freely through the inner chamber of the vial and colliding against the opposing inside wall - the impact effect. Grinding vials and balls can be fabricated from eight different materials - agate, silicon nitride, sintered corundum, zirconium, chrome steel, Cr-Ni steel, tungsten carbide, and plastic polyamide [12]. Vials and grinding balls used in this study were fabricated from tungsten carbide.

The milling process of manufacturing iron powder is described in figure 2. The raw material for the Fritsch P-6 planetary ball mill was coarse iron powder prepared by the electrochemical deposition method [13, 14]. The average particle size was 160 micrometers, particle shape is uniform, the morphology was observed by FE-SEM, purity >97.4%. The ball-to-powder weight ratio was 10:1 [12, 15]. In order to minimize oxidation, the entire operation was performed in anhydrous acetone which was filled in the mortars before milling. The samples were crushed with a setting of P6.1 mode (speed 500 rpm, each cycle time: 15 minutes of milling, 5 minutes of standing). The steps were shown in the scheme below. After certain period of milling, the mixed product and protecting solvent of each batch was removed from the mill products, a preliminary separation of the solvent was conducted in the absence of oxygen, and then, the iron powder was dried in vacuum at room temperature, round 40 - 500C for 30 minutes. The obtained iron powders were packaged and preserved in a hermetic micro-environment of very low oxygen concentration. The used acetone was an anhydrous and pure chemical analysis.

Studied iron powder samples are listed N0 – N6, in which the sample N0 is the initial material. The composition and structure of the samples were examined on the XRD, model SIEMENS D5000; surface morphology and chemical composition were determined by FE-SEM and EDX, model FESEM S-4800. Particle size distribution was determined by DLS on the HORIBA LA-950 equipment. The specific surface area and the distribution of pores were determined by the method of isothermal adsorption of nitrogen on the ASAP 2020 V3.01H. Several magnetic of milled iron powder as saturation Ms, coercivity Hc were determined by the magnetization curves M(H) [14, 15] measured at room temperature using VSM, DMS 880 model.

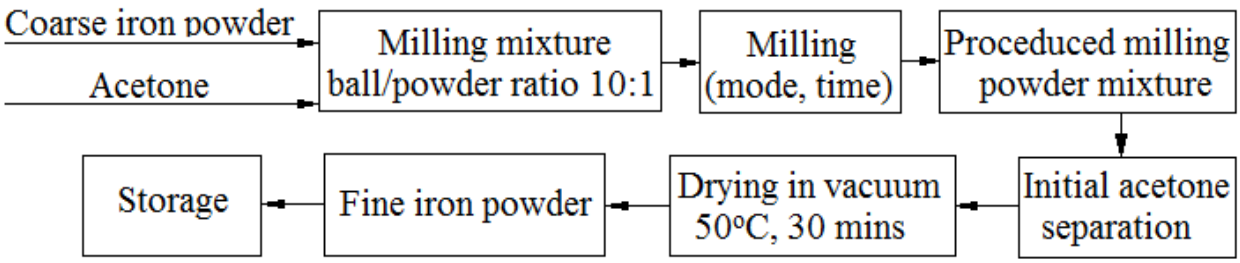

FIGURE 2. STEPS IN THE MECHANICAL GRINDING PROCESS TO PREPARE FINE IRON POWDERS

2.2 Chemicals

The chemicals used in the study include:

- FeSO4.7H2O, FeCl2.4H2O, analysis purity,
- NiSO4.6H2O, analysis purity,
- NaCl, Na2SO4, (NH4)2SO4, NH4Cl, analysis purity.
- Boric acid, citric acid, sodium citrate Na3C6H5O7, analysis purity,
- H2SO4, HCl, NaOH, NH4OH, analysis purity,
- Twice distilled water.

III. RESULTS AND DISCUSSION

3.1 Fabricating of nanoscale iron powder

Nano-sized iron powder in the range of 100-200 nm is manufactured from iron(III) oxide with average size about 150 nm (Fig.3).

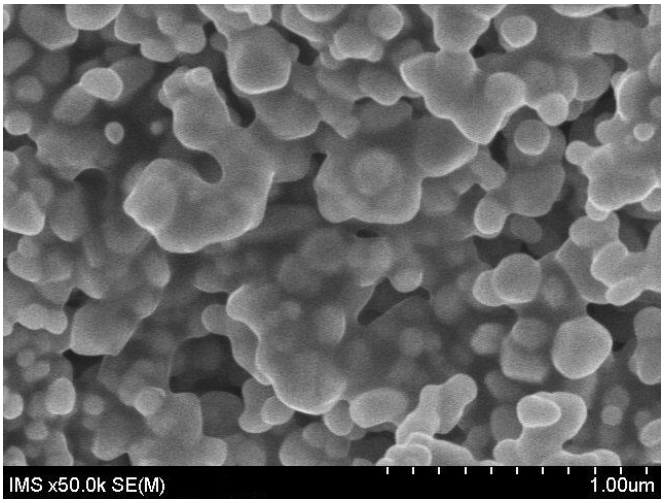

FIGURE 3. SEM IMAGES OF FABRICATED IRON POWDER

Phase component of nano iron powder sample was analyzed by X-ray diffraction, XRD pattern is shown in Figure 4. On the X-ray diffraction pattern showing the maximum diffraction peak of Fe in the value angle 2 - theta 44.7 and 65 respectively correspond to d = 2.02727 Å and d = 1.4339 Å. Beside that also the maximum diffraction peak of Fe_3O_4 however it is not clear.

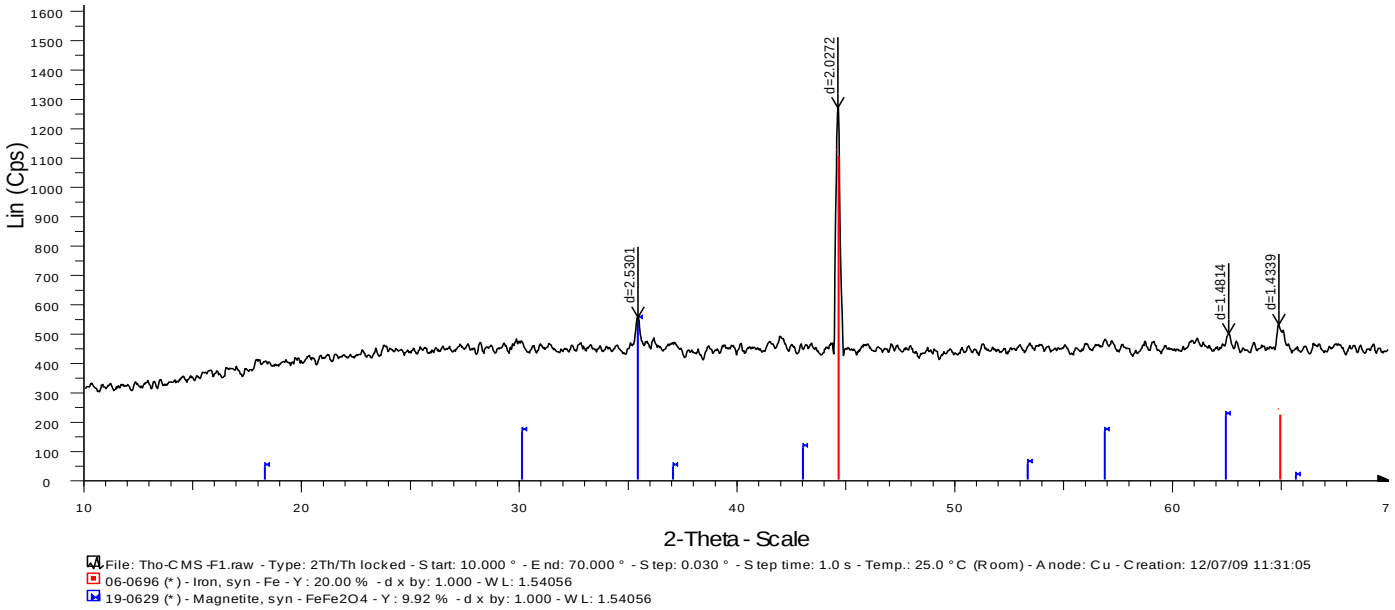

FIGURE 4 XRD PATTERN OF 100 nm Fe POWDER

The content of iron in the nano powder were analyzed using EDS method, the results showed that the iron content of over 98%.Nano iron powder is easily oxidized in a humid atmosphere, so when taking samples for analysis and in the analysis a certain percentage of iron powder was oxidized to form iron oxide FeO, reducing the purity. EDX analysis results appear only two elements are iron and oxygen, with concentrations 99.11% and 0.89% respectively, no trace of other metallic elements (Fig. 5.).

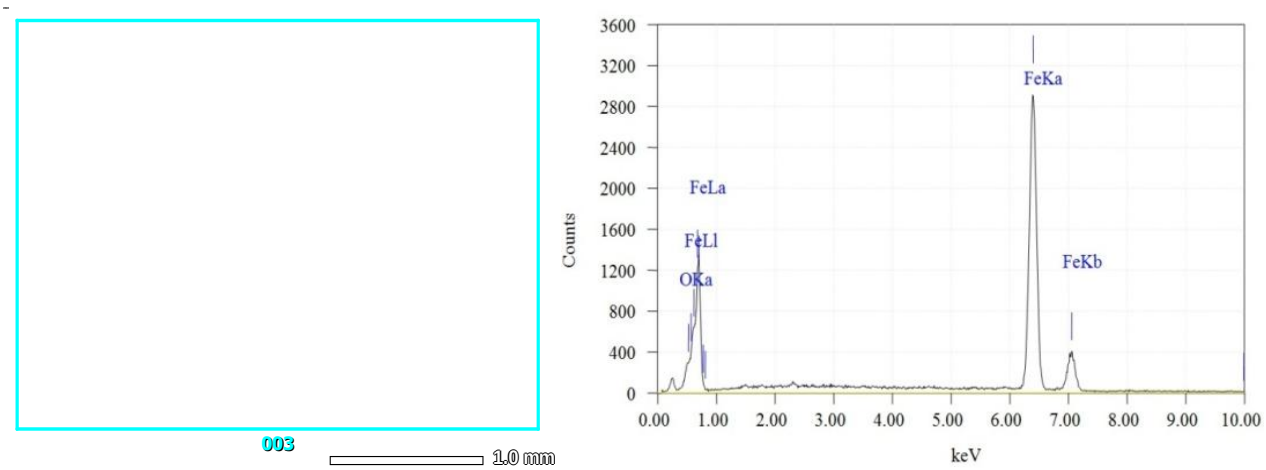

FIGURE 5. EDS SPECTRA OF NANOIRON POWDER SAMPLE AVERAGE SIZE OF 100 nm

BET plot of iron powder sample average size of 100 nm is shown in Figure 6 the analysis of the specific surface iron powder sample size of 100 nm is shown in Table 1.

From the analysis results can be seen nano iron powder was manufactured show very large surface area, 56.3625 m^2/g, more than double compared with nano iron powder that synthesized by chemical methods, promises to bring high catalytic efficiency. This shows the superiority of the reduced method by hydrogen at high temperature. Two causes of iron powder made by the hydrogen reduction method for high specific surface area that is, the first particle size of materials (iron oxides) were in nanometer, second in reduction process, oxygen atoms in oxide powder loses will leave pores in that position.

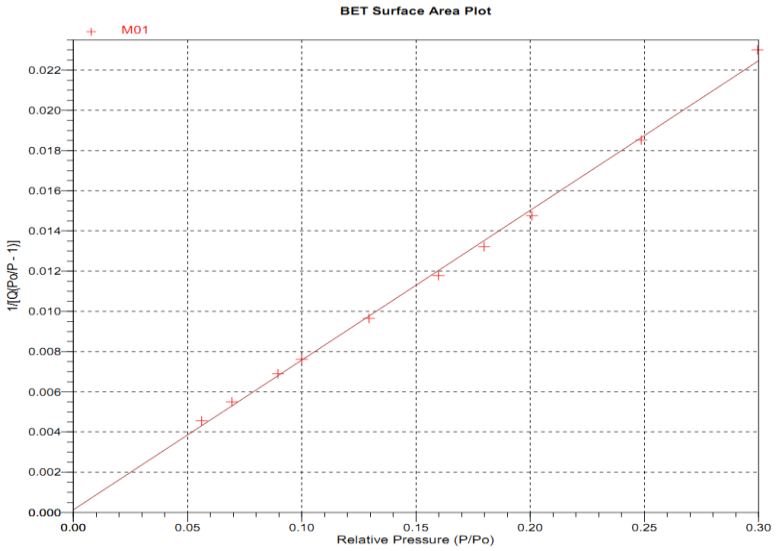

FIGURE 6. THE LINE BET OF IRON POWDER SAMPLE AVERAGE SIZE OF 100 nm

TABLE 1
THE SPECIFIC SURFACE AREA OF THE AVERAGE SAMPLE SIZE OF 100 nm

Methods	Specific surface area (m^2/g)
At P/P_0 = 0,2995	56.6823
BET	58.3625
Langmuir	89.9110
Internal capillary	6.1675
External capillary	52.1950

3.2 Fabricating of nanoscale iron on carriers

3.2.1 Morphology and surface structure

Samples after the fabrication was washed several times with distilled water, alcohol, dried and stored in sealed bags. Surface morphology of product is observed by SEM image as shown in Figure 7 and 8.

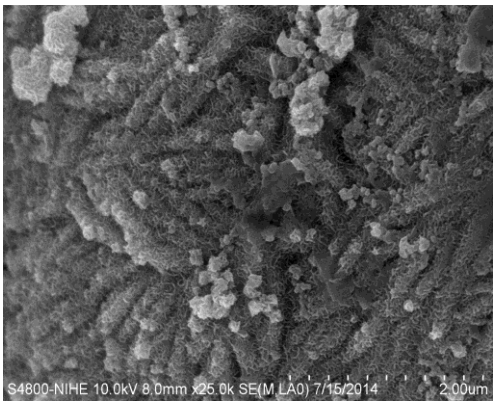

FIGURE 7. SURFACE MORPHOLOGY OF THE PRODUCT

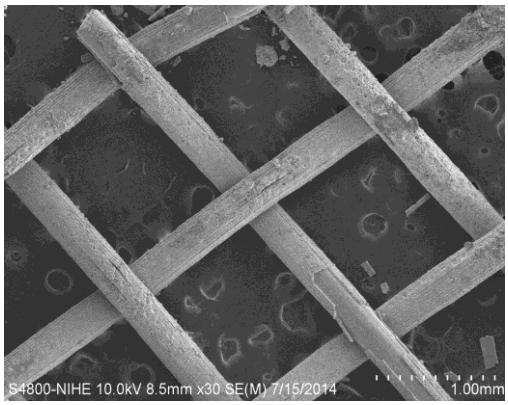

FIGURE 8. THE FORM OF THE SURFACE OF THE IRON-BASED LAYER DEPOSITED ON CARRIERS

Precipitated iron-based powder layers stick and spread over the surface are carriers (mesh). Surface precipitate layer is quite porous, the surface area greater activation.

3.2.2 The chemical composition of the *iron-based* layer

The elemental composition of iron-based layer are analyzed by EDS, composition analysis results of some samples are shown in Figure 9 and Figure 10.

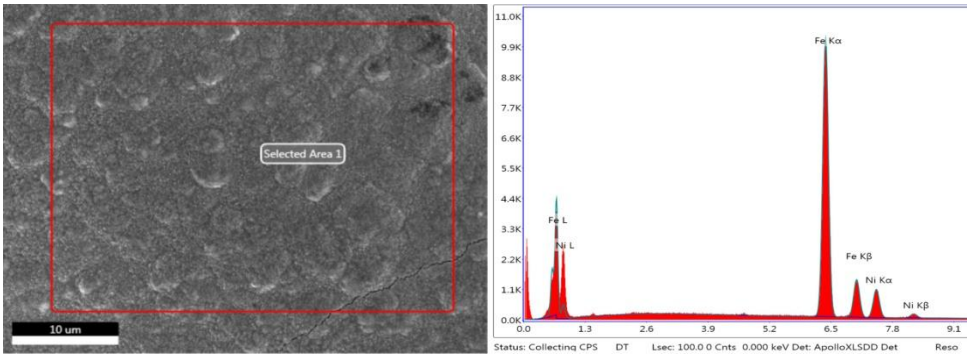

FIGURE 9. SEM AND EDS SPECTRUM OF SAMPLE, 20 MINUTES ELECTRODEPOSITE IN IRON PLATING SOLUTION WITH CURRENT DENSITY 50 A/dm2, FOLLOWED BY 1 MINUTE, 1 A/dm2 in NI PLATING SOLUTION, Fe 86.02%, Ni 13.98%.

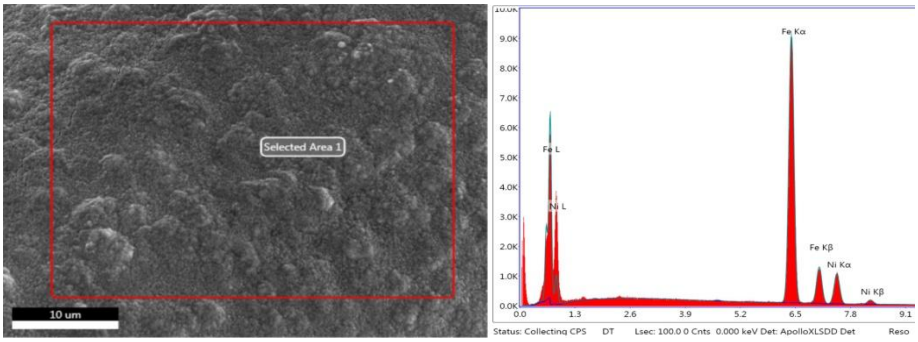

FIGURE 10. SEM AND EDS SPECTRUM OF SAMPLE, 20 MINUTES ELECTRODEPOSITED IN IRON PLATING SOLUTION WITH CURRENT DENSITY 50 A/dm^2, FOLLOWED BY 1 MINUTE, 2 A/dm^2, CONCENTRATION RATIO Fe 84.78%, Ni 15.22%.

Increasing current density the Ni content in the iron-based layer increases, the influence of the current density to Ni composition in of the iron-based layer are shown in Figure 11. Can vary composition of iron-based layer by varying current intensity or the Ni deposited time.

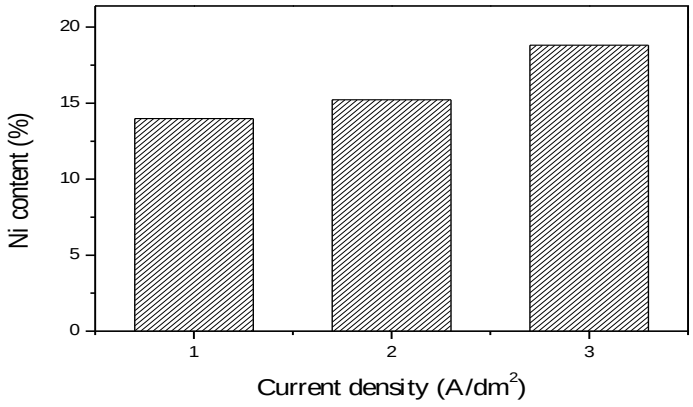

FIGURE 11. EFFECT OF CURRENT DENSITY TO *Ni* CONTENT IN THE PRODUCT LAYER, ELECTRO-DEPOSITED TIME WAS 1 MINUTE

3.3 Iron powder as grinding products

Raw material and grinding products were analyzed to determine their components by EDX analysis. The results showed that with milling time of the range from 1 to 30 hours, all of the products' purity is very high, up to 97%, table 2.

TABLE 2
CHEMICAL COMPONENT OF N0 AND N6 SAMPLE, ACHIEVED FROM EDX RESULTS.

Element	O (wt %)		Fe (wt %)		Total (wt %)	
	N0	N6	N0	N6	N0	N6
1	1.91	3.12	98.09	96.88	100	100
2	2.41	2.90	97.59	97.10	100	100
3	2.59	2.98	97.41	97.02	100	100

The observation results obtained by FE-SEM showed that the early stages of the milling process, the ion powder particles were flattened to form thin plates with small thickness, but their surface areas were large (figure 12).

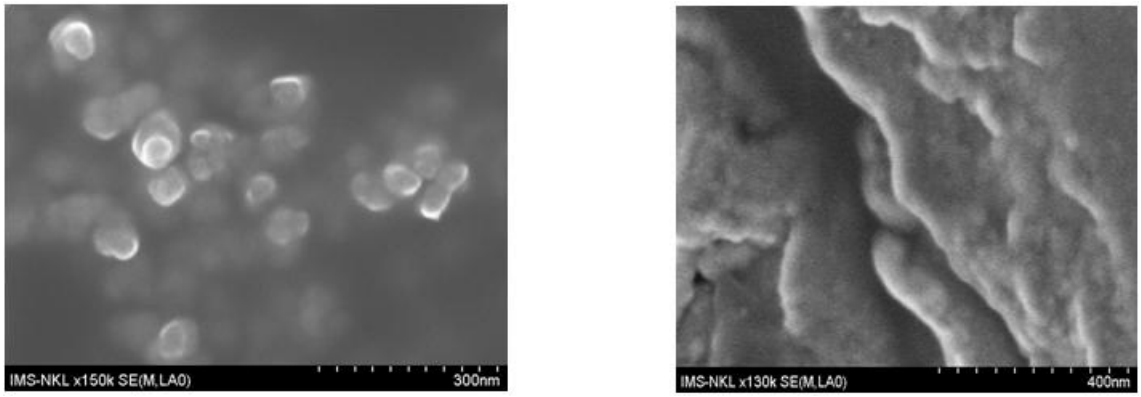

FIGURE 12. SURFACE MORPHOLOGY OF N4 SAMPLES: INDIVIDUAL PARTICLES (A), CLUSTERS (B) OF IRON POWDER

When the milling time was less than 5 hours, particles reached sizes of a few tens of micrometers.

Milling time was increased from 1 hour to 30 hours, XRD diagram with angle 2θ values in the range from 200 to 1000 of all samples from N0 to N6 have four characteristic diffraction peaks of crystalline iron of BCC α-Fe structure, the number and position of the peaks did not change for stand comparison with diffraction peaks of raw materials' spectrum. However, the width of the peaks tended to be broader, peak intensity decreased with increasing milling time, and the small amount of debris appeared, but the debris was not crystalline. X-ray diffraction diagram of the N1, N3, N5 and N6 samples were shown on figure 13.

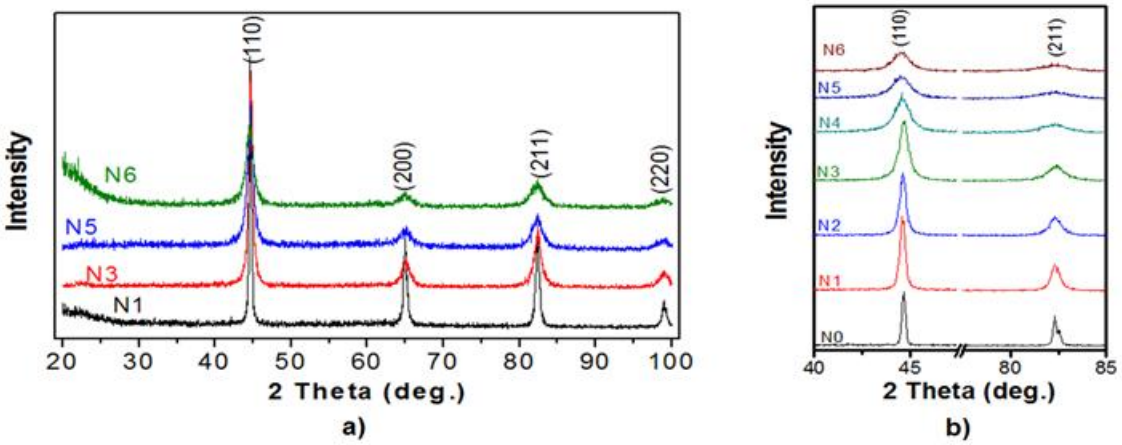

FIGURE 13. X-RAY DIFFRACTION PATTERNS OF THE SAMPLES: (A) N1, N3, N5, N6 AND (B) N0, N1 TO N6 AT 2Θ = 44.670 AND 82.320 OF TWO DIFFRACTION PEAKS CORRESPONDING TO THE PLANES (110) AND (211).

The particle size distributions of the samples N1 ÷ N6 and the original iron powder N0 sample (raw materials) were analysed by DLS technique. The results show the very strong shift and narrow area of the particle size distribution curves as a function of milling time (fig. 14-15.).

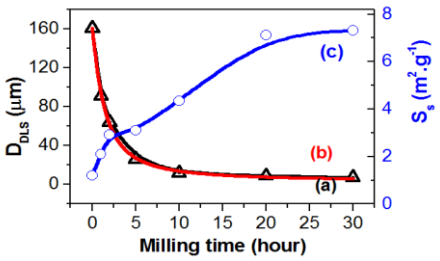

FIGURE 14. EFFECT OF MILLING TIME ON: (A) AVERAGE PARTICLE SIZE *(D_{DLS})* (B-FITTING CURVES); (C) SPECIFIC SURFACE AREA *(Ss)* OF IRON POWDER.

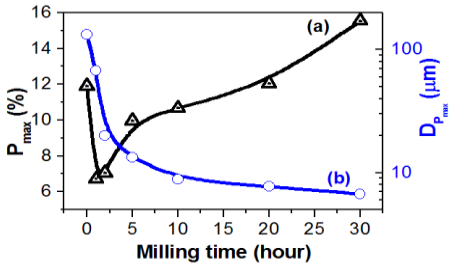

FIGURE 15. EFFECT OF MILLING TIME ON (A) THE LARGEST DISTRIBUTION (P_{max}) AND (B) THE PARTICLE SIZE AT P_{max} (D_{Pmax}) OF THE SAMPLES.

These variations were clearly observed as the milling time is increased. The results also shows that the particle size of sample N0 is in the range of 30 ÷ 400 µm, but those of N4 ÷ N6 are only in the range of 1 ÷ 30µm, meaning about 10 times smaller, as shown in figure 14-15.

Based on the results of particle size distribution, the average size of the particle D_{DLS} were determined. The specific surface area Ss of iron powder mill products determined from the isothermal nitrogen adsorption method. The relationship between the average size of D_{DLS} and Ss area with the corresponding to milling time is shown in figure 14 and 15. While milling times increased from 1 hour to 30 hours, D_{DLS} reduced from 160.77 µm to 7.21µm, and the specific surface area increased from approximately $1m^2/g$ to $7m^2/g$.

IV. CONCLUSION

Nano iron with and without a carrier have been manufactured by means of high-temperature hydrogen reduction and milling technique. Samples obtained have average particle size of about <100 nm, have high purity of 98%, single phase, the surface area of over 58 separate m_2/g, accordance BET. The nano iron product has also attached to the grating carriers by electrochemical precipitated methods in the solution containing Fe^{2+} ion and Ni^{2+} respectively. The chemical composition of the deposited layer can be adjusted by increasing the time or the current density for the Ni precipitation.

The article was completed with the support of the IES – VAST

REFERENCES

[1] Simell, P.; Kurkela, E. (1997), Biomass Gasification and Pyrolysis. Kaltschmitt, M.; Bridgwater, A.V. eds. CPL Press. Stuttgart. pp.207-217.

[2] Dang Tuyet Phuong, TranThi Kim Hoa, Vu Anh Tuan, 2010, Used Vietnam straw to produce bio-oil, Journal of Oil and Gas 10/2010, p24.

[3] Dang Tuyet Phuong, TranThi Kim Hoa, Bui Ha Linh, Hoang Yen, Vu Anh Tuan, Proceedings of the fifth nationally Scientific Conference of Catalysis and Adsorption, Haiphong (2009), pp289-302.

[4] K. Bienert, The status of the ChorenCarbo V gasification, 2nd Europ. Summ. School on Renewable Motor Fuels Warsaw, Poland, 29 – 31 August 2007

[5] N. A. Carter, R. W. Stratton, M. K. Bredehoeft and J. I. Hileman, Energy and Environmental Viability of Select Alternative Jet Fuel Pathways, 47th AIAA/ASME/SAE/ASEE Joint Propulsion Conference & Exhibit 31 July - 03 August 2011, San Diego, California

[6] Le Xuan Que, Dinh Van Kha, International conference '2nd Sustainable Energy Development, IES – VAST, 2011

[7] Simell, P.; Ståhlberg, P.; Solantausta, Y.; Hepola, J.; Kurkela, E. (1997), From Developments in Thermochemical Biomass Conversion Vol. 2, Eds: Bridgwater, A. V.; Boocock, D. G. B., Blackie, London, UK, 1103-1116.

[8] Wei-Xian Zhang, Nanoscale iron particles for Environmental Remediation, *Journal of nanoparticle Research 5* (20013) 323.

[9] Chuan Bao Wang, Wei-Xian Zhang,Synthesing nanoscale iron particles for rapid and complete dechlorination of TCE and PCBs, *Env. Science and Technology* 31, No.7(2007).

[10] http://www.nanoiron.cz/, 12/2015

[11] Le Xuan Que, Uong Van Vy, and co-authors, Scientific report of VAST project: "Stadying oxygen reducer and CO_2, SO_2 nano-absorbant, for antioxxydant presservation", ITT - VAST, Hanoi, 2012

[12] D. Dayton, A Review of the Literature on Catalytic Biomass Tar Destruction, Milestone Completion, December 2002 • NREL/TP-510-32815

[13] Suryanarayana C 2001 *Progress in Materials Science***46** p.1-184

[14] Tri L D 1987 *Electrolytic Deposition of Metals* (Hanoi: Hanoi University of Technology Publishing House).

[15] Dutz S, Hergt R, J. Mürbe J, Müller R, Zeisberger M, Andrä W, Töpfer J and Bellemann M E *2007 J. Magn. Magn. Mater*. **308** 305.